Blur Invariant Translational Image Registration for N-fold Symmetric Blurs

Matteo Pedone, Jan Flusser, *Senior Member, IEEE*, and Janne Heikkilä, *Senior Member, IEEE*

***Abstract*— In this paper, we propose a new registration method designed particularly for registering differently blurred images. Such a task cannot be successfully resolved by traditional approaches. Our method is inspired by traditional phase correlation, which is now applied to certain blur-invariant descriptors instead of the original images. This method works for unknown blurs assuming the blurring PSF exhibits an N-fold rotational symmetry. It does not require any landmarks. We have experimentally proven its good performance, which is not dependent on the amount of blur. In this paper, we explicitly address only registration with respect to translation, but the method can be readily generalized to rotation and scaling.**

***Index Terms*— Image registration, blurred images, N-fold rotation symmetry, phase correlation.**

I. Introduction

IMAGE registration is the process of overlaying two or more images of the same scene taken at different times, from different viewpoints, and/or by different sensors in such a way that the same objects should have identical spatial coordinates. Image registration is one of the most important and most frequently discussed image processing topics in the literature (see [1] for a survey). It is a crucial preprocessing step in all image analysis tasks in which the final information is obtained from a combination of various data sources (image fusion, change detection, multichannel image restoration, superresolution, etc.).

In many cases, the images to be registered are inevitably blurred. The blur may originate from camera shake, scene motion, inaccurate focus, atmospheric turbulence, sensor imperfection, low sampling density and other factors. One can encounter this situation in medical imaging where registration of images with substantially different resolution is often required (such as MRI and SPECT/PET), in remote sensing where satellite images are typically blurred due to the composite sensor PSF and atmospheric turbulence, in astronomical imaging, robotics and, last but not least, in everyday life when taking pictures using cell-phones and other low-cost devices.

Assuming the blurring factors do not change during the image formation and also assuming that the blurring is of the same kind for all pixels and all colors/gray-levels, we can describe the observed blurred image $g(\mathbf{x})$ of a scene $f(\mathbf{x})$ as a convolution

$$g(\mathbf{x}) = (f * h)(\mathbf{x}), \tag{1}$$

where the kernel $h(\mathbf{x})$ stands for the point-spread function (PSF) of the imaging system. The model (1) is a frequently used compromise between universality and simplicity – it is general enough to describe many practical situations and its simplicity allows reasonable mathematical treatment.

Registration of blurred images requires special methods. General registration methods usually do not perform well on blurred images. Feature-based methods rely on high-frequency features and components which are suppressed, modified or even missing in case of blur. The methods maximizing a similarity measure yield flat peaks which are hard to localize. Being aware of this, numerous authors pointed out that developing special registration methods is highly desirable. In the next Section, we provide a brief survey of the current approaches.

A. Existing Registration Methods for Blurred Images

Registration methods for blurred images can be, as well as the general-purpose registration methods, divided into two groups – global and landmark-based. Regardless of the particular technique, all feature extraction methods, similarity measures, and matching algorithms used in the registration process must be insensitive to image blurring.

Landmark-based blur-invariant registration methods appeared right after the first papers on moment invariants with respect to blurring [2], [3] had been published. The basic algorithm works as follows. First, significant corners and other dominant points are detected in both frames and considered as the control point candidates. To detect them, we may employ either the standard Harris detector [4] or a corner detector designed particularly for blurred images [5]. To establish the correspondence between them, a vector of moment invariants w.r.t. convolution is computed for each candidate point over its neighborhood and then the candidates are matched in the space of the invariants. Finally, we find a mapping between the images (rigid-body or affine) whose parameters are calculated via least-square fit and then resample the input image. Various authors have employed this general scenario in several modifications, differing from one

Manuscript received July 10, 2012; revised November 23, 2012, March 10, 2013, and May 24, 2013; accepted May 25, 2013. Date of publication June 14, 2013; date of current version August 13, 2013. This work was supported in part by the Czech Science Foundation under Grant P103/11/1552. The associate editor coordinating the review of this manuscript and approving it for publication was Prof. Jeffrey A. Fessler.

M. Pedone and J. Heikkilä are with the Center for Machine Vision Research, Department of Computer Science and Engineering, University of Oulu, Oulu FI-90014, Finland (e-mail: matped@ee.oulu.fi; jth@ee.oulu.fi).

J. Flusser is with the Institute of Information Theory and Automation of the Advanced Scientific Computing Research, Prague CZ-18200, Czech Republic (e-mail: flusser@utia.cas.cz).

Color versions of one or more of the figures in this paper are available online at http://ieeexplore.ieee.org.

Digital Object Identifier 10.1109/TIP.2013.2268972

another, namely by the particular invariants used as the local features. The invariants based on geometric moments can only be used for registration of blurred and mutually shifted images [3], [6], [7] and for rough registration if a small rotation is present [8]–[12]. Nevertheless, successful applications were found in matching and registration of satellite and aerial images [8], [11]–[13], as well as in medical imaging [6], [9], [10]. The discovery of blur invariants from complex moments [14] and Zernike moments [15] led to registration algorithms that are capable of handling blurred, shifted and rotated images, as has been demonstrated on satellite images [16], indoor images [17], [18] and outdoor scenes [15], [19]. Zuo [20] even combined moment blur invariants and SIFT features [21] into a single vector with weighted components but without a convincing improvement.

Global methods do not search for particular landmarks in the images. They try to estimate directly the between-image translation and rotation. Myles and Lobo [22] proposed an iterative method working well if a good initial estimate of the transformation parameters is available. Zhang *et al.* [23], [24] proposed to estimate the registration parameters by bringing the input images into a normalized (canonical) form. Since blur-invariant moments were used to define the normalization constraints, neither the type nor the level of the blur influences the parameter estimation. Kubota *et al.* [25] proposed a two-stage registration method based on hierarchical matching, where the amount of blur is considered as another parameter of the search space. Zhang and Blum [26] introduced an iterative multiscale registration based on optical flow estimation in each scale, claiming that optical flow estimation is robust to image blurring. Some registration methods were designed particularly for a certain type of blur, such as motion blur [27], out-of-focus blur [28], and camera shake blur [29]. They assume either the knowledge of the parametric form of the blurring function or of its statistical characteristics. Several authors, being motivated by superresolution applications, concentrated primarily on blur caused by insufficient resolution of the sensor. Vandewalle [30] proposed a simple translation-rotation registration method functioning in the low-frequency part of the Fourier domain in a similar way as traditional phase correlation. For heavily sub-sampled and aliased images, he recommended a variable projection method [31] which transfers the registration problem onto a minimization problem in the Fourier domain. The idea of using variable projection for blurred image registration was proposed earlier by Robinson [32]. However, Vandewalle's and Robinson's methods are robust but not exactly invariant to image blur. Since the blur can easily be modeled in the Fourier domain, Ojansivu et al. discovered certain blur-invariant properties in the spectrum phase and employed them in the registration [33], [34]. The same approach was later rediscovered by Songyuan [35] in connection with X-ray image registration.

Both landmark-based and global methods have their pros and cons. Landmark methods can typically handle more complex image distortions and can cope with only partial overlap or occlusion of the input images, as well as with space-varying blur (the blur must be constant only within the neighborhood of each landmark but can vary between landmarks). Some methods are even able to register multimodal images. On the other hand, the landmark methods require certain user-defined parameters (thresholds in corner detection, neighborhood size, number of invariants used, etc.) whose optimal values may be tricky to find and thus human interaction is usually unavoidable. The global methods are generally faster and easier to implement, which predetermines them for usage in applications where a close-to-realtime performance is required and/or where registration is supposed to be implemented in embedded systems (cameras, cell-phones, etc.). Their limitations – single modality, simple between-frame distortion (most of them allow only translation and/or rotation), the need for a large overlap of the images and the assumption of the uniform blur – might be a drawback in some applications but do not cause serious problems in registration for multichannel restoration and superresolution purposes.

B. Motivation to This Paper

The main motivation for this paper is to develop a new blur-invariant registration technique which could be subsequently used in various applications, such as multichannel restoration and superresolution algorithms. These areas are currently rapidly developing (see [36], [37]) and both inherently require registration of blurred low-resolution images.

The basic requirements the new method should meet are the following:

- *Specificity.* All methods reviewed in the previous Section either assume knowledge of the parametric form of the blurring function, which is too restrictive and not realistic, or assume *centrosymmetric* blur only, which means $h(\mathbf{x}) = h(-\mathbf{x})$. This assumption is, however, too weak – most blurring functions have a higher degree of symmetry. For instance, the PSF of out-of-focus blur is determined by the shape of the aperture. As it is formed by blades (common cameras usually have from 5 to 11 straight or slightly curved blades), it often takes a form similar to a polygon. If the aperture is fully open, then the PSF approaches a circular symmetry $h(r, \theta) = h(r)$. Also the diffraction blur is given by the aperture shape. For circular aperture, it takes a well-known form of Airy function; however, for a polygonal aperture, the corresponding PSF is more complicated (see Fig. 1 for some examples of non-circular defocus and diffraction blur). The registration method designed specifically for a particular symmetry of the blurring PSF should exhibit better performance than general approaches.
- *Image type and between-image distortion.* We consider images of identical or similar modalities with an unknown shift, which is supposed to be the main geometric difference between them. One or both images may be blurred; in case both are blurred their PSF's generally differ from each other.
- *Speed.* We envisage a future implementation in embedded systems; thus, the method should be fast and easy to implement on DSP. The latest development moves in this direction [38].

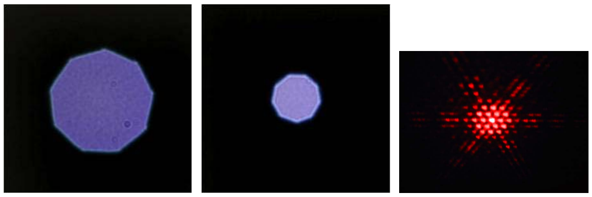

Fig. 1. Real examples of the PSF's originating from wrong focus (left and middle). Depicted images are photographs of a bright point. The objective has nine blades which determine the shape of the aperture. Diffraction PSF on an aperture formed by six blades (right).

- *Accuracy.* Registration accuracy is not a critical issue here. The method should namely avoid large misregistrations. The subsequent restoration/superresolution algorithms can efficiently compensate for small errors up to 1-2 pixels by overestimating the PSF's support [39].

Taking the above requirements into account, we concentrate on global methods working in the Fourier domain. We present a novel registration method which is invariant to blurring of the input image(s) by an unknown N-fold symmetric PSF. The proposed method was partially inspired by

- Traditional phase correlation for non-blurred images by De Castro and Morandi [40].
- Ojansivu's work [34], [41] on blur-invariant phase correlation for centrosymmetric PSF's.
- Flusser's et al's work on moment invariants w.r.t. convolution with N-fold symmetric kernels [42], [43].

This paper is organized as follows: in the next Section we recall the phase correlation method, its invariant version for centrosymmetric PSF, projection operators and introduce invariants to N–fold symmetric PSF in the Fourier domain. Section III forms the core of this paper and introduces a registration method invariant to N–fold symmetric blurs. The experiments in Section IV illustrate its performance.

II. Preliminaries

In this Section, we introduce some terms and properties which we later employ in the new method and in comparative experiments.

A. Notation

In this paper, we deal solely with 2D images. We use vector notation $\mathbf{x} = (x, y)$ for the coordinates in the spatial domain and similarly $\mathbf{u} = (u, v)$ in the frequency domain. We employ the traditional definition of the Fourier transform:

$$\mathcal{F}\{f\}(\mathbf{u}) \equiv F(\mathbf{u}) = \int_{R^2} f(\mathbf{x}) e^{-2\pi i(\mathbf{u}\cdot\mathbf{x})} d\mathbf{x}.$$

We also introduce the rotation operator R_α which rotates the image by angle α and is defined as

$$(R_\alpha f)(\mathbf{x}) = f(\mathrm{R}_\alpha \mathbf{x}) \ , \ \mathrm{R}_\alpha = \begin{pmatrix} \cos\alpha & -\sin\alpha \\ \sin\alpha & \cos\alpha \end{pmatrix}$$

The rotation operator commutes with the Fourier transform

$$\mathcal{F}\{R_\alpha f\} = R_\alpha F.$$

B. Phase Correlation

Phase correlation introduced by De Castro and Morandi [40] is among the most popular global registration methods because of its simplicity, speed, and robustness to varying illumination. In most cases, it works well even if the images have only a partial overlap. Its intuitive meaning is that it performs correlation of whitened images which is similar to correlation of edges. Actual implementation works in Fourier domain where it takes advantage of the Fourier Shift Theorem [44] saying that the Fourier transforms of two mutually shifted images differ from each other by the phase shift only. Let $g(\mathbf{x}) = f(\mathbf{x} - \Delta)$. Then

$$G(\mathbf{u}) = e^{-2\pi i \mathbf{u}\cdot\Delta} F(\mathbf{u})$$

and we get for the cross-power spectrum

$$S(\mathbf{u}) \equiv \frac{F \cdot G^*}{|F| \cdot |G|}(\mathbf{u}) = e^{2\pi i \mathbf{u}\cdot\Delta}. \tag{2}$$

By means of the inverse Fourier transform, we obtain a single peak located exactly in $-\Delta$:

$$\mathcal{F}^{-1}\{S\}(\mathbf{x}) = \delta(\mathbf{x} + \Delta).$$

Why does not the phase correlation work well for blurred images? Let $g'(\mathbf{x}) = (f * h)(\mathbf{x} - \Delta)$. Then the cross-power spectrum S' of f and g' is

$$S'(\mathbf{u}) = S(\mathbf{u}) e^{i\phi(\mathbf{u})},$$

where $\phi(\mathbf{u})$ is the phase of $H(\mathbf{u})$. Hence, $\mathcal{F}^{-1}\{S'\}(\mathbf{x})$ does not yield a single peak but rather produces a pattern resembling the (shifted) gradient of $h(\mathbf{x})$ (see Fig. 2). Except for trivial cases, such as those of a constant-phase H, the recovering of Δ is difficult. The situation becomes even more complicated if *both* images are blurred, each of them differently.

Ojansivu's extension of the phase correlation [34], [41] assumes that h is centrosymmetric, i.e. $h(\mathbf{x}) = h(-\mathbf{x})$. Then $H(\mathbf{u})$ is real (i.e. $\phi(\mathbf{u}) = 0$ or π) and the square of the "blurred" cross-power spectrum equals the square of the clear cross-power spectrum

$$S'(\mathbf{u})^2 = S(\mathbf{u})^2 \cdot e^{2i\phi(\mathbf{u})} = S(\mathbf{u})^2. \tag{3}$$

The inverse FT of $S'(\mathbf{u})^2$ returns a single peak in -2Δ independently on the particular h. Unfortunately, this approach cannot be generalized in a straightforward manner to other symmetries.

C. N-Fold Rotational Symmetry

In this section, we define functions with *N–fold rotational symmetry* (N-FRS). Later in this paper, the assumption of N–fold rotational symmetry will be imposed on the blurring PSF's. As already mentioned, numerous real-life PSF's exhibit this kind of symmetry. Diffraction and out-of-focus blur were discussed above, the atmospheric turbulence has a symmetry with $N = \infty$ and also the shake and motion PSF's – provided that the exposure time is relatively short so the speed of shake/motion is constant and trajectory is linear – are of this kind with $N = 2$.[1]

[1] For constructing invariants, it is sufficient that the PSF is N-fold symmetric with respect to its centroid, which is the case of the motion blur.

A function h is said to have N-FRS if it repeats itself when it rotates around the origin by $\alpha_j = 2\pi j/N$ for all $j = 1, \ldots, N$. In polar coordinates this means that

$$h(r, \theta) = h(r, \theta + \alpha_j) \qquad j = 1, \ldots, N$$

and, equivalently, in terms of rotation operators

$$R_j h = h,$$

where $R_j \equiv R_{\alpha_j}$.

Particularly, $N = 1$ means no symmetry in a common sense and $N = 2$ denotes the central symmetry. We use this definition not only for finite N, but also for $N = \infty$ which stands for the functions having a circular symmetry $h(r, \theta) = h(r)$. We denote a set of all functions as N–fold rotation symmetry as S_N. An interesting property of S_N is that it is closed to three basic between-function operations – addition, multiplication and convolution – and also to the Fourier transform. If $h \in S_N$, then also $H \in S_N$ (if it exists).

D. Invariants to N-Fold Symmetric Blur

Flusser et al. [43] introduced the projection operator P_N onto S_N as an average of rotation operators:

$$P_N f = \frac{1}{N} \sum_{j=1}^{N} R_j f.$$

This operator decomposes a function into an N-fold symmetric part and "the rest", similarly to the 1-D case, where one can decompose any function into even and odd parts. It holds $P_N f \in S_N$ for any f. Operator P_N commutes with the Fourier transform:

$$\mathcal{F}\{P_N f\} = P_N F.$$

In [43], the projection operators are employed to define invariants with respect to image blurring in the following way: let us consider an image f which was blurred according to (1) with an unknown PSF $h \in S_N$. Then, the ratio

$$I_N(\mathbf{u}) = \frac{\mathcal{F}\{f\}(\mathbf{u})}{\mathcal{F}\{P_N f\}(\mathbf{u})} = \frac{F}{P_N F}(\mathbf{u}) \tag{4}$$

does not depend on h at all. The proof implies from the relation

$$I_N^{(f*h)} = \frac{\mathcal{F}\{f * h\}}{\mathcal{F}\{P_N(f * h)\}} = \frac{F \cdot H}{P_N(F \cdot H)} = \frac{N \cdot F \cdot H}{\sum_{j=1}^{N} R_j F \cdot R_j H}.$$

Since $H \in S_N$, we have $R_j H = H$ for any $j = 1, \ldots, N$. Consequently,

$$I_N^{(f*h)} = \frac{F \cdot H}{H \cdot P_N F} = \frac{F}{P_N F} = I_N^{(f)}$$

□

The blur invariant I_N has an interesting intuitive interpretation. It is a ratio of two Fourier transforms which may be interpreted as a deconvolution of the image f with the kernel $P_N f$. This "deconvolution" exactly eliminates the symmetric part of f. I_N can be viewed as the Fourier transform of a *primordial image* (although such an image may not exist in a common sense), which plays a role of a canonical form of f. Since the primordial image is the same for all images differing from one another by an N-fold symmetric convolution, its arbitrary feature is an N-fold blur invariant.[2]

III. N-Fold Blur-Invariant Phase Correlation

A. Phase Correlation of Primordial Images

At first sight, it seems natural to apply standard phase correlation to primordial images and in this way to obtain a blur-invariant registration method. However, the cross-power spectrum

$$C(\mathbf{u}) = \frac{I_N^{(f)} I_N^{(g)*}}{\left|I_N^{(f)}\right| \left|I_N^{(g)}\right|}$$

produces neither a single peak, nor any other easy-to-detect pattern in $\mathcal{F}^{-1}\{C\}(\mathbf{x})$. The main reasons are that, unlike "conventional" image spectra, the magnitude $|I_N|$ is not preserved if f is shifted and also that projection operators do not commute with a shift. The relation between $C(\mathbf{u})$ and Δ can still be derived and (at least theoretically) used for estimating the registration parameters. However, this process, when implemented numerically, is not robust. Its sensitivity to non-complete overlap of the images and to noise makes it unreliable.

In the next Section, we propose an alternative blur invariant registration method which is based on the same principle but is more suitable for detecting the between-image shift.

B. Phase Correlation Between Separated N-Fold Invariants

In the previous Section, we have discussed the problems arising from the approach of estimating the shift between two blurred images f and g using the strategy of computing phase correlation of their primordial images. We now present an alternative method whose properties will enable us to obtain a robust estimate of the translational shift between f and g.

We start by observing that the invariant expressed in (4) is not the only possible formulation of an N-fold blur invariant. Let's introduce the following operators:

$$K_j^{(f)}(\mathbf{u}) = \frac{F(\mathbf{u})}{F(\mathrm{R_j}\mathbf{u})} \quad j = 1, \ldots, N \tag{5}$$

(We dropped the index N for simplicity.) It is straightforward to verify that $K_j^{(f)}$ is invariant to image blurring. For an image f blurred by an N-fold symmetric PSF h, we have

$$K_j^{(f*h)}(\mathbf{u}) = \frac{F(\mathbf{u})H(\mathbf{u})}{F(\mathrm{R_j}\mathbf{u})H(\mathrm{R_j}\mathbf{u})} = K_j^{(f)}(\mathbf{u}).$$

Under a translation of the image, the operator K_j preserves its magnitude

$$|K_j^{(f(\mathbf{x}-\Delta))}| = |K_j^{(f)}|$$

while its phase is changed such that

$$\frac{K_j^{(f)}}{K_j^{(f(\mathbf{x}-\Delta))}} = e^{-i\mathbf{u}\cdot(\mathrm{R_j^T}\Delta - \Delta)}$$

[2]Moment invariants w.r.t. N-fold blur introduced in [42] are "almost" the moments of the primordial image.

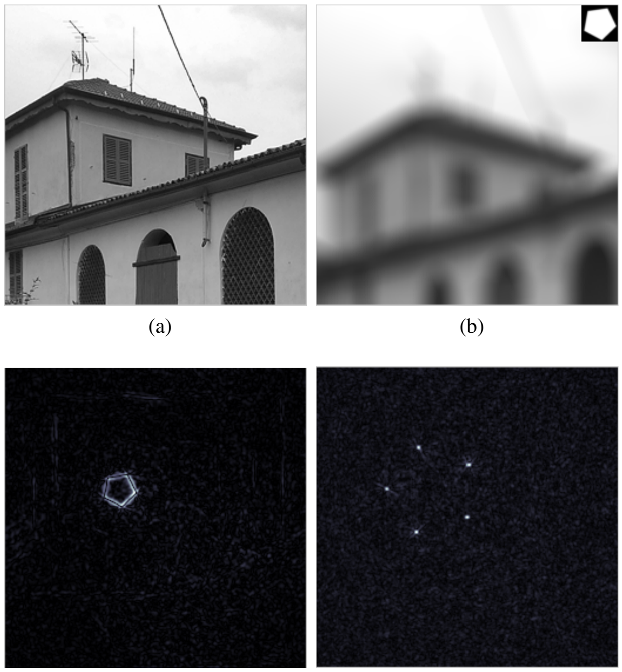

(a) (b) (c) (d)

Fig. 2. Registration by N-fold phase correlation of the reference and blurred images (a)-(b). On the top-right corner of (b), the PSF is depicted. (c) IFT of the correlation spectrum obtained by ordinary phase correlation. The peak lies somewhere at the "edges" of the PSF, while the true shift is in the center of the PSF. (d) IFT of $C = \sum_{j=1}^{N} C_j$ for $N = 5$. The center of the circle determines the shift between the images.

for any shift Δ. We now calculate the cross-power spectrum $C_j(\mathbf{u})$ between two invariants $K_j^{(f)}$, $K_j^{(g)}$ where $g(\mathbf{x}) = (f * h)(\mathbf{x} - \Delta)$:

$$C_j(\mathbf{u}) = \frac{K_j^{(f)} K_j^{(g)*}}{|K_j^{(f)}||K_j^{(g)}|} = \frac{K_j^{(f)} K_j^{(g)*}}{|K_j^{(g)}|^2} = = \frac{K_j^{(f)}}{K_j^{(f(\mathbf{x}-\Delta))}} = e^{-i\mathbf{u}\cdot(\mathrm{R}_j^{\mathrm{T}}\Delta - \Delta)} \tag{6}$$

Equation (6) proves that each $\mathcal{F}^{-1}\{C_j\}$ yields a delta function located at intervals of $2\pi j/N$ radians along a circle centered at $\mathbf{x} = -\Delta$ and passing through the origin (see Fig. 2). This allows us to detect the coordinates of each of the $N-1$ peaks (the one for $j = N$ is always at the origin) and then to fit the peaks by a circle. The center of such circle directly represents the shift between the two images.

The invariants $K_1^{(f)}, \ldots, K_N^{(f)}$ are dependent, thus they encode redundant information. It holds always that $K_N^{(f)}(\mathbf{u}) = 1$, and moreover, we have

$$K_1^{(f)} \cdot (R_1 K_j^{(f)}) = K_{j+1}^{(f)}$$

which means that it is theoretically sufficient to use one *generator* $K_1^{(f)}$ to calculate the other $N-1$ invariants. Due to this redundancy, we theoretically could recover Δ just from a single C_j but for the sake of robustness it is better to use all of them.

C. Fitting a Circle

Detecting the peak in each $\mathcal{F}^{-1}\{C_j\}$ is simple just by identifying the maximum value, so we find a peak location $\mathbf{p}_j$ such that $\mathcal{F}^{-1}\{C_j\}(\mathbf{p}_j) > \mathcal{F}^{-1}\{C_j\}(\mathbf{x})$, for all other $\mathbf{x} \in \mathbb{Z}^2$. Theoretically, it should be the only non-zero value there. In practice, this is not the case due to finite precision, but still the peak significantly exceeds the other values in $\mathcal{F}^{-1}\{C_j\}$ and is easy to locate. After detecting all the peaks $\mathbf{p}_1, \mathbf{p}_2, \ldots, \mathbf{p}_{N-1}$ a crucial step is to fit the circle, the center of which determines the shift parameters. Note that always $\mathbf{p}_N = \mathbf{0}$ and hence we constrain the circle to pass through the origin in any case.

In data fitting, minimization of an L_2-norm is mostly used, which leads to a popular least-square fit. This is well justified if the measurement errors show a normal distribution. However, our experiments indicate that in our case this assumption is not valid. We face two kinds of errors. The first one, caused by a finite-precision calculation and discretized coordinates, leads to negligible sub-pixel errors. The second kind of errors is, however, much more serious. Our theoretical derivation of the method was done in a continuous domain for images having infinite support. In practice, we always work with discrete finite-supported images. Discrete FT exhibits well-known periodic properties and the discrete Fourier shift theorem (which provides the theoretical background for our method) is valid for periodic shifts only. This may produce ambiguities and consequently errors in peak locations. A large shift to the right can be interpreted as a small shift to the left, and vice versa. Note that the diameter of the circle equals the double shift, so the circle often appears to be "folded" in the finite coordinate plane. There is no way to determine, for a given peak, whether it was detected in its correct position or in a position of "modulo image size". This ambiguity produces errors in peak locations that are not normally distributed, but rather can be modeled by a heavy-tailed exponential distribution with a small exponent. Hence, in this case the L_2-norm is not an appropriate measure of a goodness of fit. We have to use another L_p-norm for $p < 1$ which is more robust to outliers. Based on our experimental investigation, we choose $p = 0.2$ which exhibits a satisfactory performance. We did not observe significant changes in performance when we set p within the range $0.1 \leq p \leq 0.5$. Fitting the circle actually means finding its center $\mathbf{c}$ (the radius r is given by the constraint as $r = ||\mathbf{c}||$) such that

$$E_p = \left(\sum_{j=1}^{N-1} \left| \|\mathbf{p_j} - \mathbf{c}\| - r \right|^p \right)^{\frac{1}{p}} \tag{7}$$

is minimized. Fig. 3 shows the difference between minimization of E_2 and $E_{0.2}$.

D. Implementation Details

When implementing the proposed method, one has to take into account certain differences between discrete finite-support images and continuous infinite-support ones. We already mentioned those arising from using DFT; however there are also some other issues requiring certain care.

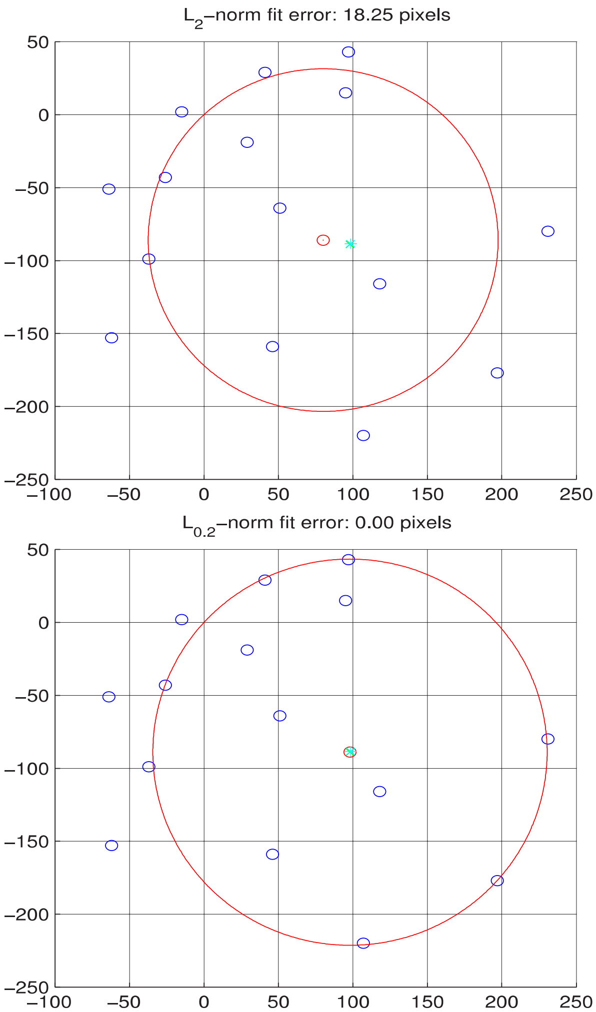

Fig. 3. Sixteen peaks detected in an experiment (blue rings) fitted by a circle which minimizes the error in L_2-norm (left) and in $L_{0.2}$-norm (right). The star is a ground-truth center (i.e. the ground-truth image shift), the red ring is a center of the fitted circle (i.e. the detected image shift). The fit by $L_{0.2}$-norm yields a perfect result, unlike the L_2-norm fit.

- *Padding.* In order not to lose any data when rotating the image and constructing $R_j f$, the image support must be enlarged and the image appropriately padded. Since mirror as well as periodic paddings might lead to registration ambiguities, we just replicate the image borders.
- *Interpolation.* Rotated coordinates are generally non-integer, so we use bilinear interpolation when rotating the padded images. Higher-order interpolation does not bring any noticeable improvement.
- *Suppression of boundary effects.* Discrete phase correlation (both traditional as well as blur-invariant) suffers from the sensitivity to boundary effect – if the patterns in the images are not very prominent, the method tends to "register" the image borders, i.e. it yields false shift parameters one or both of them being zero. To prevent this, we smooth the border areas of the images by a Gaussian filter.

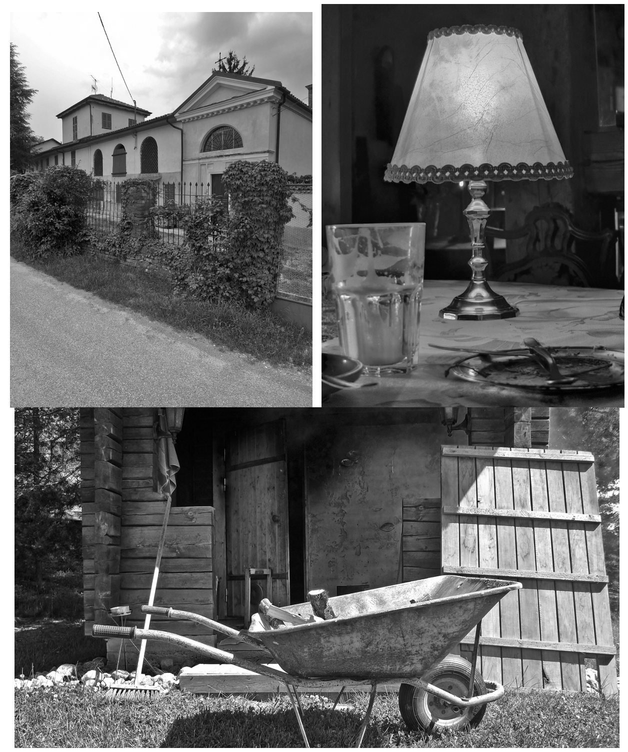

Fig. 4. The three original images from which the patches were randomly extracted and blurred.

Having implemented the method, we can now proceed to test it in experiments in the following Section.

IV. Experiments

In order to test the performance of the proposed method, we performed two different kinds of experiments: the first one was carried out on simulated data with different levels of computer-generated blur and translation, while in the second experiment, a real out-of-focus blur and translations were present. We now describe these two experiments in detail.

A. Computer-Generated Blur, Translation and Noise

The aim of this experiment was to test the performance of the proposed method in a controlled environment where the ground truth is precisely known. This approach enabled us to evaluate the success rate as a function of the amount of blur, of the image overlap and noise. We also compared our method to the traditional phase correlation.

We used three different images (Fig. 4) and their blurred versions, obtained by convolving the originals with an almost circular point-spread function (actually we used a polygon with $N = 32$) with a user-defined radius. From each of the three sharp images, ten patches of size 255×255 pixels were randomly selected, yielding a total of 30 test images. For each of these 30 reference sharp images, a "partner patch" of the same size was extracted from the blurred large image in such a way that the reference and partner patches had a given percentage of mutual overlap. The actual coordinates of the partner patch were selected randomly. This procedure was repeated for all blurs from radius 0 to 15 pixels. Clearly, high overlaps

TABLE I

PERFORMANCE OF THE N-FOLD PHASE CORRELATION, $N = 8$, WITH VARIOUS AMOUNTS OF OVERLAP FROM 90% TO 40% (IN THE COLUMNS) AND VARIOUS BLUR RADIUS FROM 0 TO 15 PIXELS (IN THE ROWS). IN EACH BOX, THE NUMBER OF MISREGISTERED IMAGE PAIRS (OUT OF 30) IS DISPLAYED

	0	**1**	**2**	**3**	**4**	**5**	**6**	**7**	**8**	**9**	**10**	**11**	**12**	**13**	**14**	**15**
90%	*0*	*0*	*0*	*0*	*0*	*0*	*0*	*0*	*0*	*0*	*0*	*0*	*0*	*0*	*0*	*0*
80%	*0*	*0*	*0*	*0*	*0*	*0*	*0*	*0*	*0*	*0*	*0*	*0*	*0*	*0*	*0*	*0*
70%	*0*	*0*	*0*	*0*	*0*	*0*	*0*	*0*	*0*	*0*	*0*	*0*	*0*	*0*	*0*	*0*
60%	*0*	*0*	*0*	*0*	*0*	*0*	*0*	*0*	*0*	*0*	*0*	*0*	*0*	*0*	*0*	*0*
50%	*3*	*0*	*0*	*1*	*1*	*0*	*2*	*0*	*2*	*0*	*0*	*2*	*0*	*3*	*0*	*0*
40%	*6*	*6*	*5*	*5*	*5*	*4*	*8*	*3*	*9*	*7*	*4*	*5*	*6*	*5*	*7*	*6*

TABLE II

PERFORMANCE OF ORDINARY PHASE CORRELATION WITH VARIOUS AMOUNTS OF OVERLAP FROM 90% TO 40% (IN THE COLUMNS) AND VARIOUS BLUR RADIUS FROM 0 TO 15 PIXELS (IN THE ROWS). IN EACH BOX THE NUMBER OF MISREGISTERED IMAGE PAIRS (OUT OF 30) IS DISPLAYED

	0	**1**	**2**	**3**	**4**	**5**	**6**	**7**	**8**	**9**	**10**	**11**	**12**	**13**	**14**	**15**
90%	*0*	*0*	*0*	*0*	*3*	*30*	*30*	*30*	*30*	*30*	*30*	*30*	*30*	*30*	*30*	*30*
80%	*0*	*0*	*0*	*0*	*0*	*30*	*30*	*30*	*30*	*30*	*30*	*30*	*30*	*30*	*30*	*30*
70%	*0*	*0*	*0*	*0*	*3*	*30*	*30*	*30*	*30*	*30*	*30*	*30*	*30*	*30*	*30*	*30*
60%	*0*	*0*	*0*	*0*	*2*	*30*	*30*	*30*	*30*	*30*	*30*	*30*	*30*	*30*	*30*	*30*
50%	*0*	*0*	*0*	*0*	*3*	*30*	*30*	*30*	*30*	*30*	*30*	*30*	*30*	*30*	*30*	*30*
40%	*0*	*1*	*0*	*1*	*2*	*29*	*30*	*30*	*30*	*30*	*30*	*30*	*30*	*30*	*30*	*30*

TABLE III

MEDIAN SHIFT ERROR IN PIXELS (**BOLD** TEXT) OF ORDINARY PHASE CORRELATION, AND MEDIAN ABSOLUTE DEVIATION (*Italic* TEXT) WITH DIFFERENT AMOUNTS OF OVERLAP (ROWS) AND BLUR RADII (COLUMNS). THE STATISTICS WERE COMPUTED FROM 30 IMAGE PAIRS FOR EACH ENTRY OF THE TABLE. THE ANALOGOUS STATISTICS FOR N-FOLD PHASE CORRELATION WITH $N = 8$ YIELDED A TABLE FULL OF ZEROS WHICH IS NOT DISPLAYED

	0	**1**	**2**	**3**	**4**	**5**	**6**	**7**	**8**	**9**	**10**	**11**	**12**	**13**	**14**	**15**
90%	**0**	**0**	**0**	**0**	**1**	**2.23**	**3.6**	**4.47**	**5.83**	**6.7**	**7.81**	**8.6**	**10**	**10.79**	**12.04**	**12.8**
	0	*0*	*0*	*0*	*0.7*	*0*	*0*	*0*	*0.17*	*0.3*	*0.22*	*0.22*	*0.19*	*0.2*	*0.35*	*0.19*
80%	**0**	**0**	**0**	**0**	**0**	**2.23**	**3.6**	**4.47**	**5.83**	**6.7**	**7.81**	**8.6**	**9.84**	**10.81**	**11.7**	**12.8**
	0	*0*	*0*	*0*	*0*	*0*	*0*	*0*	*0.16*	*0.33*	*0.19*	*0.11*	*0.35*	*0.18*	*0.33*	*0.23*
70%	**0**	**0**	**0**	**0**	**0**	**2.23**	**3.6**	**4.47**	**5.83**	**6.7**	**7.81**	**8.6**	**9.89**	**10.79**	**11.7**	**12.72**
	0	*0*	*0*	*0*	*0*	*0*	*0.39*	*0.28*	*0.17*	*0.3*	*0.19*	*0.11*	*0.1*	*0.16*	*0.33*	*0.23*
60%	**0**	**0**	**0**	**0**	**0**	**2.23**	**3.6**	**4.47**	**5.65**	**6.7**	**7.81**	**8.77**	**10**	**10.77**	**11.7**	**12.8**
	0	*0*	*0*	*0*	*0*	*0*	*0*	*0.22*	*0.27*	*0.3*	*0.19*	*0.22*	*0.12*	*0.14*	*0.3*	*0.27*
50%	**0**	**0**	**0**	**0**	**1**	**2.23**	**3.6**	**4.47**	**5.83**	**6.85**	**7.81**	**8.6**	**9.89**	**10.79**	**11.7**	**12.8**
	0	*0*	*0*	*0*	*0.2*	*0*	*0.19*	*0*	*0.25*	*0.21*	*0.19*	*0.11*	*0.22*	*0.09*	*0.31*	*0.23*
40%	**0**	**0**	**0**	**0**	**1**	**2.23**	**3.6**	**4.47**	**5.83**	**6.7**	**7.71**	**8.6**	**9.94**	**10.81**	**11.7**	**12.8**
	0	*0*	*0*	*0*	*0*	*0.23*	*0*	*0.34*	*0.17*	*0.33*	*0.34*	*0.35*	*0.24*	*0.18*	*0.33*	*0.39*

correspond to small displacements between the patches, while for low overlaps, the shift which is to be recovered by the registration becomes larger. We considered six different levels of overlap: 90%, 80%, 70%, 60%, 50%, and 40%. The overlaps higher than 90% are not challenging (100% overlap means no shift) and the overlaps below 50% are difficult to register by any global registration technique. Hence, we generated 2,880 pairs of patches of various overlap and blur.

Each pair was registered (which means here that the between-patch shift was estimated) by the new method described in Section III. In this simulated experiment, the blur has almost circular symmetry, so N should be chosen "sufficiently large" (the theoretical value is $N = \infty$, actual ground-truth value is $N = 32$, but we set $N = 8$ in this experiment to avoid a perfect match which is not realistic in practice). A larger N would provide slightly better results but at the expense of computing complexity, while choosing a smaller N would decrease the performance slightly. For comparison, traditional phase correlation was applied as well. Since the ground-truth shift vector $\mathbf{s}_{gt}$ between the patches was known, it is possible to calculate the registration error ε as

$$\varepsilon = \left\| \mathbf{s}_{gt} - \hat{\mathbf{s}} \right\|$$

where $\hat{\mathbf{s}}$ stands for the estimated shift. We consider any registration, yielding an error $\varepsilon > 1$, to be a misregistration. We measure the performance of the algorithm by counting the number of misregistrations for all possible combinations of blur radii and overlaps. The results are shown in Tables I and II. Furthermore, we include two robust statistics to assess the accuracy of the methods: the median error, and the median absolute deviation (Table III). The latter is simply defined as $median_i(|\epsilon_i - median_j(\epsilon_j)|)$, where ϵ_i is the shift error for to the i-th image pair. We justify the use of these robust statistics by noticing that when the N-fold phase correlation algorithm fails, the output estimated shift is essentially random following an approximately Gaussian distribution with large variance, while "correct" registrations follow an approximately exponential distribution with high rate parameter (see Fig. 6).

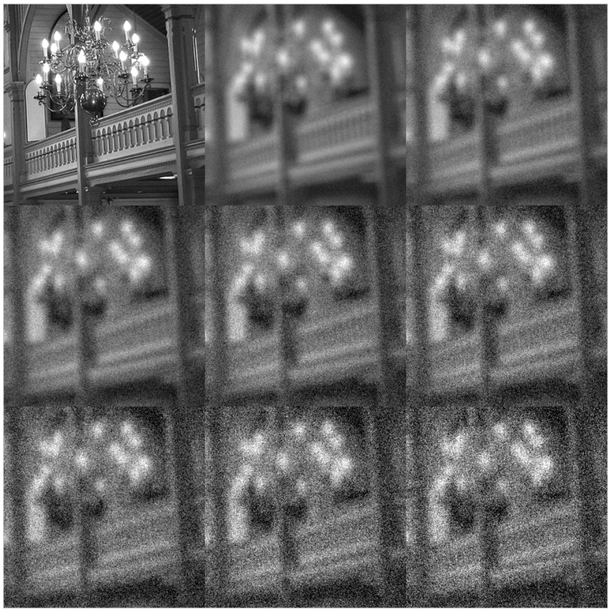

Fig. 5. The original image *(top left)* and eight noisy instances with the amounts of noise used in the experiment.

TABLE IV
ROBUSTNESS OF THE N-FOLD PHASE CORRELATION, $N = 8$, WITH RESPECT TO ADDITIVE GAUSSIAN NOISE. OVERLAP OF THE PATCHES 70%, BLUR RADIUS 7 PIXELS

Gaussian Noise σ	**5**	**10**	**15**	**20**	**25**	**30**	**35**	**40**
Misregistrations (out of 100)	*0*	*5*	*9*	*11*	*19*	*31*	*38*	*43*

Any measure based on the mean squared error would not be appropriate for assessing accuracy, as it would introduce a considerable bias due to the random shift error occurring in cases of misregistrations.

It is apparent that ordinary phase correlation was capable of tolerating very low amounts of blur only. This is in accordance with the theory; in fact, the maximum peak extracted from the correlation spectrum typically lies somewhere at the "edges" of the PSF centered in the location corresponding to the true shift (Fig. 2c). This is further confirmed by the statistics reported in Table III where the accuracy of ordinary phase correlation appears to decrease linearly with greater blur radii. However, even if we incorporated this knowledge into the algorithm, it would not be sufficient to recover the shift parameters. Thus, the registration error is approximately proportional to the radius of the blurring PSF.

On the other hand, the proposed N-fold blur invariant phase correlation is designed to address this drawback, and in fact, it did not yield any misregistration for overlaps larger than 50% and only a few for 50%, which is a perfect performance. If the overlap is only 40%, some of the peaks which are fitted by a circle fall beyond the support we are working on and, due to the periodicity of DFT, they appear in locations which are "modulo the image size". This happens particularly to the correlation peaks extracted from C_j using (6), when j is close to $N/2$. Although the $L_{0.2}$ fit is robust to outliers, it fails if such points are too many. In our experiment the mean

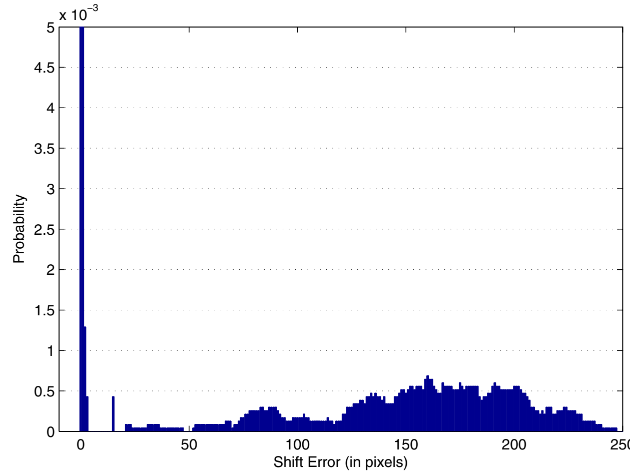

Fig. 6. Distribution of the shift error in pixels obtained using N-fold blur invariant phase correlation with $N = 8$, for 1,024 image pairs, overlap 40%, and blur radius 15. The probability of the first bin is approximately 0.18.

misregistration rate in case of 40% overlap is 6 out of 30 trials (this rate is nearly independent on the blur amount) which is still much better than that of traditional phase correlation. The median error and the median absolute deviation obtained with the N-fold phase correlation were remarkably all zero for all combinations of overlap/blur radius. This essentially means that the registrations yielded either an error of 0 pixel, or a random shift, but the random shifts are treated as outliers by these robust statistics.

An additional experiment was carried out in order to test the robustness of the proposed method with respect to noise. In this experiment, 100 patch pairs were randomly selected as described above. The overlap was kept fixed at 70%, and the blur radius was set to 7 pixels. The blurred images were degraded by different levels of additive white Gaussian noise. Since the pixel intensities of the images lie within the range [0..255], the noise standard deviations used were 5, 10, 15, 20, 25, 30, 35, and 40. Fig. 5 depicts the effect of the noise levels used in the experiment. The proposed method was utilized to align the sharp images with the blurred and noisy versions. The results, demonstrating reasonable robustness of the method, are shown in Table IV.

B. Real Camera Translation and Out-of-Focus Blur

See Figs. 9 and 10 for the result of this experiment. In this experiment, two pairs of images were taken with a hand-held standard compact camera. The blur was introduced intentionally by changing the focus settings. In each pair, we changed settings between acquisitions and we also moved the camera slightly, which resulted in differently blurred and mutually shifted images. Assuming the PSF's are close to circular, we chose $N = 16$ and applied the N-fold phase correlation to register the images. In order to demonstrate one of the possible applications of this registration technique, we used the registered images as an input for the multichannel blind-deconvolution algorithm described in [39]. In both cases, the resulting deblurred images have much better appearance than the blurred inputs, with almost no artifacts, which is

TABLE V

ROBUSTNESS OF THE METHOD WITH RESPECT TO THE CHOICE OF THE FOLD NUMBER. NUMBER OF MISREGISTERED IMAGE PAIRS OUT OF 100, COUNTED FOR DIFFERENT SETTINGS OF N. THE TRUE PSF HAS 4-FOLD SYMMETRY. THE BIGGEST ERRORS ARE FOR THE CHOSEN FOLD NUMBERS 3 AND 5, RESPECTIVELY (SEE THE TEXT FOR EXPLANATION)

Fold number applied	**2**	**3**	**4**	**5**	**16**	**17**	**31**
Misregistrations (overlap 80%)	*2*	*29*	*0*	*12*	*3*	*2*	*3*
Misregistrations (overlap 50%)	*21*	*68*	*1*	*65*	*20*	*15*	*15*

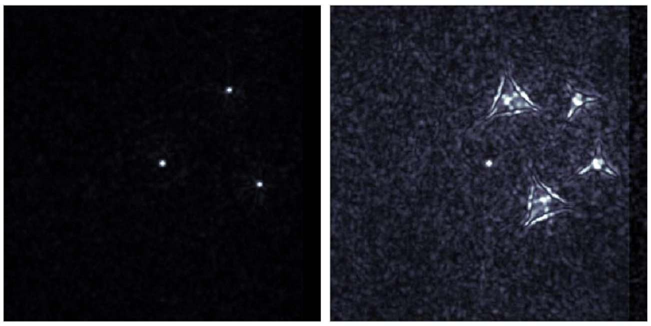

Fig. 7. Registration of images blurred by a triangular PSF. The correct choice $N = 3$ results in three isolated peaks, while the incorrect one $N = 5$ leads to a composite pattern. Fitting of the circle is less accurate in the latter case.

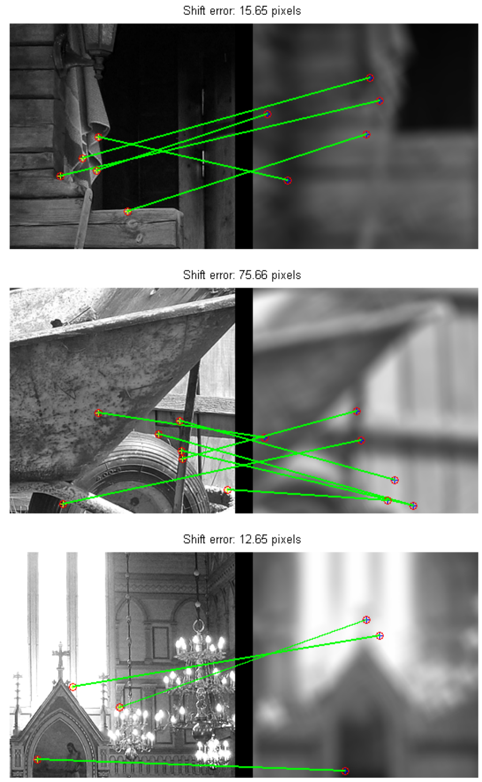

Fig. 8. Some examples of matched SURF features in the experiment with the calculated registration error.

an indication that the registration was accurate enough (since there is no ground truth, we cannot directly evaluate the error). The deconvolution algorithm also yields as a by-product the estimated PSF's. One can see they are approximately but not exactly circularly symmetric. The violation of symmetry may originate from second-order errors of the optics and also from estimation errors. In spite of that, the registration algorithm has proven sufficient robustness to such deviations from the assumed PSF shape.

C. Choice of N

The only user defined parameter of the method is the fold number of the PSF. Choosing a proper N, which in practice is often unknown, might be a tricky problem. Ideally, it should be deduced from the physical model of the blurring source or from other prior information. We may also try to estimate N directly from the blurred image by analyzing its spectral patterns or the response to an ideal bright point or a spot of a known shape, if available. If none of the above is applicable and the user chooses N randomly, a danger of failure is imminent. Intuitively, if we overestimate N in order to have more points for the fit, the invariance property of the method is lost and some peaks appear on false positions. On the other hand, some users might underestimate it to be on the safe side (they might choose for instance $N = 2$ instead of the correct value $N = 6$). This would always lead to loss of robustness and sometimes could also violate the invariance, depending on the actual and chosen N.

In order to estimate the impact of a wrong choice of N, the following experiment was carried out. We randomly selected 25 patches of 256×256 pixels from four reference images, for a total of 100 patches, and blurred them with a 4-fold square-shaped PSF having size 31×31 pixels. To incorporate sampling errors as well, we rotated the PSF by 15 degrees before applying the blur. Then we registered the patches to the reference patch using the proposed method for the fold numbers 2, 3, 4, 5, 16, 17, and 31, respectively. When $N = 2$, no circle fit can be used, and this particular case is treated as in [34]. We ran this experiment twice, first the overlap between the reference and each blurred patch was 80% and in the second round the overlap was only 50%. The results are summarized in Table V.

We can see that the method yields almost perfect results for $N = 4$ and tolerates a wrong choice of the fold number in certain cases. Let us denote the chosen fold number as M. This tolerance depends mainly on the distance between the spectral peaks produced by the correct N and those by M. Note, that the "width" of the M-peaks is inversely proportional to the distance from the nearest N-peak. The following situations may occur:

- If $N > M$ and $M|N$, then M is theoretically correct (all M-peaks coincide with some N-peaks) but might be less robust. Therefore, we have two misregistrations for $M = 2$.
- If $N > M$ and are not coprime, then at least some M-peaks coincide with some N-peaks. This is worse than the previous case but still may lead to the correct result. This configuration did not occur in our experiment.
- If $N > M$ and are coprime. No peaks (except the origin) coincide. The goodness of fit of the M-peaks depends

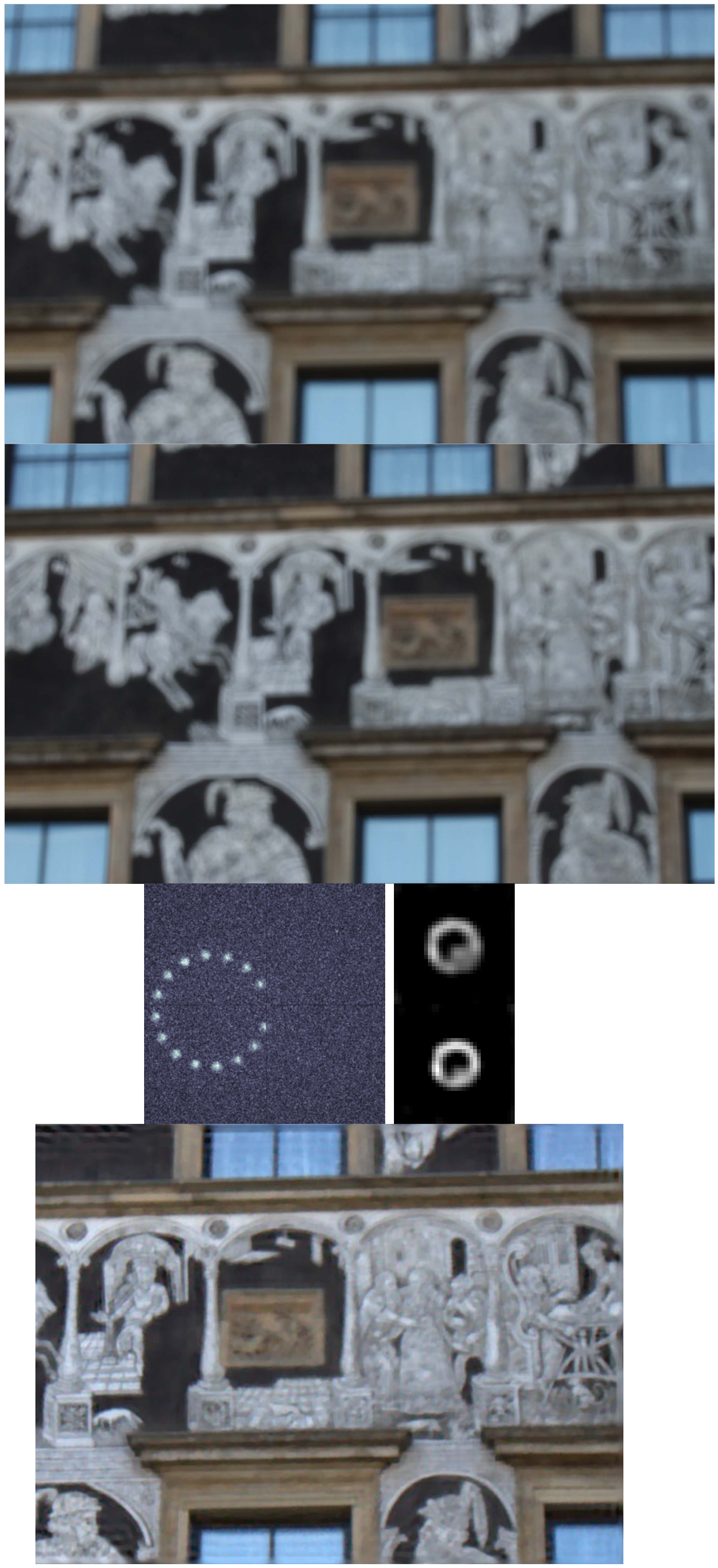

Fig. 9. The first pair of blurred images to be registered (top), the spectral peaks (middle left), the estimated PSF's (middle right), and the result of the multichannel deconvolution [39] performed after the registration (bottom).

on how close they are to the N-peaks. The distance to an N-peak not only says how far an M-peak is from the correct position, but also says how spread it is. The closer to a correct location, the sharpest peak, which is easier to detect and fit than the spread one. The minimum distance between the peaks is given by $d = \min(|aN - bM|)$,

Fig. 10. The second pair of blurred images to be registered (top), the spectral peaks (middle), the estimated PSF's (bottom left), and the result of the multichannel deconvolution [39] performed after the registration (bottom right). The absence of visible artifacts illustrates high registration accuracy.

where the minimization is calculated over the integers $1 \le b \le N-1$ and $1 \le a \le M-1$. The minimal d is large if N and M are small; the worst case ever is $N = 3$ and $M = 2$. In our experiment, the worst configuration was $N = 4$ and $M = 3$, which led to the highest number of misregistrations.

- If $N < M$ and $N|M$, then all N-peaks are found (they coincide with some M-peaks), and although there will be other wrong peaks, the robust circle fit might still yield correct results in this case.
- If $N < M$ and are not coprime, then at least some N-peaks are found correctly, which still may lead to the correct result. However, the false M-peaks may violate the fit.
- If $N < M$ and are coprime, no peaks (except the origin) coincide, and there is a high probability of failure,

particularly for small N and M. See the case $M = 5$ in the experiment.

To summarize, although the correct choice of the fold number is desirable, the method provides a good chance of finding correct registration parameters even in some cases of an incorrect choice, namely if M is a multiple or divisor of N. One of the worst cases is depicted in Fig. 7. The true PSF had 3-fold symmetry, but we set $N = 5$, which led to the smoothing of the spectral peaks. The patterns which appear instead of the isolated points are analogous to the pattern we observe when applying traditional phase correlation to blurred images. The local maxima could be anywhere on this pattern.

Another questionable choice of N arises if both images are blurred, but their PSF's have different fold numbers (say N_1 and N_2). Since the parameter N in the algorithm is just one and joint for both of them, the theoretically optimal choice is to take N as the greatest common divisor of N_1 and N_2. If N_1 and N_2 are coprime, the task is not correctly solvable. In such a case, we recommend to choose either N_1 or N_2 depending on which blur is more severe.

From the discussion above, it is clear that the worst scenarios are when the true N and the chosen M are coprime and both *small*. If absolutely no knowledge about N can be assumed, nor any interaction by the user, one can at least alleviate the problem by choosing a large M, and as a rule-of-thumb, we may suggest $M = 16$. Alternatively, the user could manually try few commonly occurring N and check the sharpness of the peaks as an indicator of a good choice.

D. Comparison With SURF-Based Registration

We compared our N-fold blur invariant phase correlation method with another registration method of a different nature that uses detection of local features and matches the control points in order to estimate the translational shift between two images. For our experiment, we chose the popular SURF feature detector [45] which is known to be fairly robust to moderate amounts of blur [46]. We used 23 image pairs of the size 255×255 and 60% overlap between them. The direction of the shift was chosen randomly. One image of the pair was blurred with a 4-fold symmetric PSF of 31×31 pixels. For our proposed method, we used $N = 16$. For the detection and matching of the control points, we used the detector-descriptor scheme presented in [45] and we adopted the upright variant of SURF called U-SURF which, according to its authors, is more robust when rotation invariance is not required. In order to estimate the (x, y) shift from the matching features of the two images we use a RANSAC-based approach to reduce the effect of outliers due to wrong matches. The proposed N-fold phase correlation method yielded always a perfect registration with a subpixel error. The method based on U-SURF and RANSAC was unable to produce any correct registration for all the image pairs in the experiment. For the latter approach, the mean of the Euclidean distances between the estimated shift and the ground-truth shift was 44.78 pixels. The best performance with U-SURF resulted in an error of approximately 12 pixels, and was obtained for six image pairs. The worst registrations occurred with four image pairs and yielded an error of more than 100 pixels. This experiment shows the weaknesses of popular approaches based on matching features. To be applicable in the case of blurred images, such feature detectors would have to be invariant to blurring. However, common point detectors like SURF and SIFT calculates second-order derivatives which are smoothed as the image is blurred. Moreover, the information extracted by local descriptors from small patches of a moderately blurred image, is often insufficient to guarantee a correct match with a corresponding patch of a differently blurred image if such descriptors are not blur invariant. As seen in Fig. 8, the error in registration is apparently caused by the high amount of wrong matches of U-SURF features.

E. Computational Speed

In our experiments, we used a MATLAB implementation of the algorithm, and we achieved an average computational time for performing N-fold blur invariant phase correlation of approximately $1.36(N-1)P$, where P is the average running time required by ordinary phase correlation, and N is the chosen fold number.

V. Conclusion and Discussion

In this paper, we proposed an original registration method designed particularly for registering blurred images. Such a task appears quite often in various applications and, as demonstrated, cannot be successfully resolved by traditional approaches. Our method belongs to the global landmark-free registration techniques and was inspired by the well-known phase correlation. It works for unknown blurs assuming the PSF's exhibit N-fold rotational symmetry. We proved experimentally its good performance which is not dependent on the amount of blur. It can, of course, be applied to non-blurred images as well, but in that case, it loses its advantage over the standard techniques. It should be noted that there exist (rare) cases of space-invariant blur where our method is not applicable because the PSF has no symmetry, for instance a motion blur along a curved trajectory and high-frequency vibration/shake blur with changing parameters during the acquisition. The method is also not rigorously applicable in the case of space-variant PSF.

The implementation of the method is simple and efficient, it consists only of two Fourier transforms, $N - 1$ inverse Fourier transforms, $2N$ rotations and few other simple steps. This could enable its embedded implementation on the camera chips in the future.

The most serious problem when implementing the method comes from the combination of a finite support of the images, low overlap (i.e. large shift) and the periodic properties of Fourier transform. Various strategies could be adopted in order to overcome this problem. One strategy could be that of using only the N-fold invariants of lowest order, e.g. $K_j^{(\cdot)}$ for $j = 1, \ldots, J$, and $J < N - 1$. In this way, fewer points are available for the circle fitting, but the peaks produced will be closer to the origin, hence, more likely to lie within one half of the correlation spectrum. Another strategy would be that of performing registration using ordinary phase correlation as the first step, in order to increase the overlap between the image pairs. Then the second step would be performed using N-fold invariant phase correlation to correct the registration error due to blur, and obtain the exact displacement. Such a two-step approach would however obviously increase the computational cost of the registration algorithm and may also fail when performing the first stage.

The version presented in this paper deals with between-image shift only. This is, however, not a serious drawback for two reasons. Firstly, we target mainly at the applications where the images are acquired shortly one after another (such as in multichannel deconvolution) so the difference is almost solely translation. Secondly, the extension to rotation and scaling, if needed, is a straightforward technical matter. One can use the same approach which is well-known from the standard phase correlation [40]: by using polar (or log-polar) mapping rotations (and scalings) are transformed into translations. In this sense, there is no difference between our method and standard phase correlation. As a rule, certain implementation problems arise due to the unequal sampling in the polar domain, but that is another topic irrelevant to blurring.

We can see future challenges in this field, namely in adapting this method also to other PSF symmetries such as dihedral symmetry. Extension to 3D images is in principle possible, but we have to keep in mind that in 3D the set of symmetries is much richer than in 2D and a straightforward extension of the 2D theory, even if restricted only to shift, is impossible.

Acknowledgment

The authors would like to thank Dr. F. Šroubek for providing some test images and the code for the MBD.

References

[1] B. Zitová and J. Flusser, "Image registration methods: A survey," *Image Vis. Comput.*, vol. 21, no. 11, pp. 977–1000, 2003.

[2] J. Flusser, T. Suk, and S. Saic, "Recognition of blurred images by the method of moments," *IEEE Trans. Image Process.*, vol. 5, no. 3, pp. 533–538, Mar. 1996.

[3] J. Flusser and T. Suk, "Degraded image analysis: An invariant approach," *IEEE Trans. Pattern Anal. Mach. Intell.*, vol. 20, no. 6, pp. 590–603, Jun. 1998.

[4] C. Harris and M. Stephens, "A combined corner and edge detector," in *Proc. 4th Alvey Vis. Conf.*, 1988, pp. 147–151.

[5] B. Zitová, J. Kautsky, G. Peters, and J. Flusser, "Robust detection of significant points in multiframe images," *Pattern Recognit. Lett.*, vol. 20, no. 2, pp. 199–206, 1999.

[6] Y. Bentoutou, N. Taleb, M. Chikr El Mezouar, M. Taleb, and J. Jetto, "An invariant approach for image registration in digital subtraction angiography," *Pattern Recognit.*, vol. 35, no. 12, pp. 2853–2865, 2002.

[7] I. Makaremi and M. Ahmadi, "Wavelet domain blur invariants for image analysis," *IEEE Trans. Image Process.*, vol. 21, no. 3, pp. 996–1006, Mar. 2012.

[8] Y. Bentoutou, N. Taleb, K. Kpalma, and J. Ronsin, "An automatic image registration for applications in remote sensing," *IEEE Trans. Geosci. Remote Sens.*, vol. 43, no. 9, pp. 2127–2137, Sep. 2005.

[9] Y. Bentoutou and N. Taleb, "Automatic extraction of control points for digital subtraction angiography image enhancement," *IEEE Trans. Nuclear Sci.*, vol. 52, no. 1, pp. 238–246, Feb. 2005.

[10] Y. Bentoutou and N. Taleb, "A 3-D space–time motion detection for an invariant image registration approach in digital subtraction angiography," *Comput. Vis. Image Understand.*, vol. 97, no. 1, pp. 30–50, 2005.

[11] S. X. Hu, Y.-M. Xiong, M. Z. W. Liao, and W. F. Chen, "Accurate point matching based on combined moment invariants and their new statistical metric," in *Proc. ICWAPR 2007*, pp. 376–381.

[12] Y. Bentoutou, N. Taleb, A. Bounoua, K. Kpalma, and J. Ronsin, "Feature based registration of satellite images," in *Proc. 15th Int. Conf. DSP 2007*, 2007, pp. 419–422.

[13] Z. Liu, J. An, and L. Li, "A two-stage registration angorithm for oil spill aerial image by invariants-based similarity and improved ICP," *Int. J. Remote Sens.*, vol. 32, no. 13, pp. 3649–3664, 2011.

[14] J. Flusser and B. Zitová, "Combined invariants to linear filtering and rotation," *Int. J. Pattern Recognit. Artif. Intell.*, vol. 13, no. 8, pp. 1123–1136, 1999.

[15] B. Chen, H. Shu, H. Zhang, G. Coatrieux, L. Luo, and J. L. Coatrieux, "Combined invariants to similarity transformation and to blur using orthogonal Zernike moments," *IEEE Trans. Image Process.*, vol. 20, no. 2, pp. 345–360, Feb. 2011.

[16] J. Flusser, B. Zitová, and T. Suk, "Invariant-based registration of rotated and blurred images," in *Proc. IGARSS 1999*, Jun., pp. 1262–1264.

[17] J. Flusser, J. Boldyš, and B. Zitová, "Moment forms invariant to rotation and blur in arbitrary number of dimensions," *IEEE Trans. Pattern Anal. Mach. Intell.*, vol. 25, no. 2, pp. 234–246, Feb. 2003.

[18] B. Zitová and J. Flusser, "Estimation of camera planar motion from blurred images," in *Proc. ICIP 2002*, Sep., pp. 329–332.

[19] X. Dai, H. Zhang, H. Shu, L. Luo, and T. Liu, "Blurred image registration by combined invariant of legendre moment and Harris-Laplace detector," in *Proc. 4th PSIVT 2010*, pp. 300–305.

[20] Z. X. D. Xiubin, L. Limin, S. Huazhong, and S. JiFeng, "M-SIFT: A new descriptor based on legendre moments and SIFT," in *Proc. 3rd ICMV 2010*, pp. 183–186.

[21] D. G. Lowe, "Distinctive image features from scale-invariant keypoints," *Int. J. Comput. Vis.*, vol. 60, no. 2, pp. 91–110, 2004.

[22] Z. Myles and N. V. Lobo, "Recovering affine motion and defocus blur simultaneously," *IEEE Trans. Pattern Anal. Mach. Intell.*, vol. 20, no. 6, pp. 652–658, Jun. 1998.

[23] Y. Zhang, C. Wen, and Y. Zhang, "Estimation of motion parameters from blurred images," *Pattern Recognit. Lett.*, vol. 21, no. 5, pp. 425–433, 2000.

[24] Y. Zhang, C. Wen, Y. Zhang, and Y. C. Soh, "Determination of blur and affine combined invariants by normalization," *Pattern Recognit.*, vol. 35, no. 1, pp. 211–221, 2002.

[25] A. Kubota, K. Kodama, and K. Aizawa, "Registration and blur estimation methods for multiple differently focused images," in *Proc. Int. Conf. Image Process.*, vol. 2. 1999, pp. 447–451.

[26] Z. Zhang and R. Blum, "A hybrid image registration technique for a digital camera image fusion application," *Inf. Fusion*, vol. 2, no. 2, pp. 135–149, 2001.

[27] K. V. Arya and P. Gupta, "Registration algorithm for motion blurred images," in *Proc. 6th Int. Conf. Adv. Pattern Recognit.*, 2007, pp. 186–190.

[28] X. Fang, B. Luo, B. He, and H. Wu, "Feature based multi-resolution registration of blurred images for image mosaic," *Int. J. CAD/CAM*, vol. 9, no. 1, pp. 37–46, 2009.

[29] L. Yuan, J. Sun, L. Quan, and H.-Y. Shum, "Blurred/non-blurred image alignment using sparseness prior," in *Proc. 11th ICCV 2007*, pp. 1–8.

[30] P. Vandewalle, S. Susstrunk, and M. Vetterli, "A frequency domain approach to registration of aliased images with application to super-resolution," *EURASIP J. Appl. Signal Process.*, vol. 2006, pp. 1–14, Jan. 2006.

[31] P. Vandewalle, L. Sbaiz, and M. Vetterli, "Registration for super-resolution: Theory, algorithms, and applications in image and mobile video enhancement," in *Super-Resolution Imaging*, P. Milanfar, Ed. Boca Raton, FL, USA: CRC Press, 2011, pp. 155–186.

[32] D. Robinson, S. Farsiu, and P. Milanfar, "Optimal registration of aliased images using variable projection with applications to super-resolution," *Comput. J.*, vol. 52, no. 1, pp. 31–42, 2009.

[33] V. Ojansivu and J. Heikkilä, "A method for blur and affine invariant object recognition using phase-only bispectrum," in *Proc. ICIAR*, vol. LNCS 5112. 2008, pp. 527–536.

[34] V. Ojansivu and J. Heikkilä, "Image registration using blur-invariant phase correlation," *IEEE Signal Process. Lett.*, vol. 14, no. 7, pp. 449–452, Jul. 2007.

[35] S. Tang, Y. Wang, and Y. Wei Chen, "Blur invariant phase correlation in X-ray digital subtraction angiography," in *Proc. IEEE/ICME Int. Conf. Complex Med. Eng., 2007*, May, pp. 1715–1719.

[36] K. E. Patrizio Campisi, *Blind Image Deconvolution: Theory and Applications*. Boca Raton, FL, USA: CRC Press, 2007.

[37] P. Milanfar, *Super-Resolution Imaging*. Boca Raton, FL, USA: CRC Press, 2011.

[38] F. Šroubek, J. Kamenický, and J. Flusser, "Denoising, deblurring, and superresolution in mobile phones," *Proc. SPIE*, vol. 7873, p. 78730I, Jan. 2011.
[39] F. Šroubek and J. Flusser, "Multichannel blind deconvolution of spatially misaligned images," *IEEE Trans. Image Process.*, vol. 14, no. 7, pp. 874–883, Jul. 2005.
[40] E. de Castro and C. Morandi, "Registration of translated and rotated images using finite Fourier transform," *IEEE Trans. Pattern Anal. Mach. Intell.*, vol. 9, no. 5, pp. 700–703, Sep. 1987.
[41] V. Ojansivu, "Blur invariant pattern recognition and registration in the Fourier domain," Ph.D. dissertation, Dept. Electr. Inf. Eng., Univ. Oulu, Oulu, Finland, 2009.
[42] J. Flusser, T. Suk, and B. Zitová, *Moments and Moment Invariants in Pattern Recognition*. New York, NY, USA: Wiley, 2009.
[43] J. Flusser, T. Suk, J. Boldyš, and B. Zitová, "Blur invariants and projection operators," in *Proc. 10th IASTED Conf. Signal Process., Pattern Recognit. Appl. SPPRA*, 2013, pp. 305–312.
[44] R. N. Bracewell, *The Fourier Transform and Its Applications*. New York, NY, USA: McGraw-Hill, 1965.
[45] H. Bay, T. Tuytelaars, and L. Van Gool, "SURF: Speeded up robust features," in *Proc. ECCV 2006*, pp. 404–417.
[46] L. Juan and O. Gwun, "A comparison of SIFT, PCA-SIFT and SURF," *Int. J. Image Process.*, vol. 3, no. 4, pp. 143–152, 2009.

Matteo Pedone received the M. Sc. degree in computer science from the "Sapienza" University of Rome, Rome, Italy, in 2007. He is currently pursuing the Ph.D. degree with the Center for Machine Vision Research, University of Oulu, Oulu, Finland. His current research interests include computer vision, computational photography, statistical signal processing, differential geometry, and Clifford algebra.

Jan Flusser (M'93–SM'03) received the M.Sc. degree in mathematical engineering from Czech Technical University, Prague, Czech Republic, in 1985, the Ph.D. degree in computer science from the Czechoslovak Academy of Sciences, Prague, in 1990, and the D.Sc. degree in technical cybernetics in 2001. Since 1985, he was with the Institute of Information Theory and Automation, Academy of Sciences of the Czech Republic, Prague. From 1995 to 2007, he was the Head of the Department of Image Processing. Since 2007, he has been the Director of the Institute. He is a Full Professor of computer science with the Czech Technical University, Prague, and Charles University, Prague, where he gives undergraduate and graduate courses on Digital Image Processing, Pattern Recognition, and Moment Invariants and Wavelets. His current research interests include moments and moment invariants, image registration, image fusion, multichannel blind deconvolution, and super-resolution imaging. He has authored or co-authored more than 150 research publications, including the monograph *Moments and Moment Invariants in Pattern Recognition* (Wiley, 2009), tutorials and invited/keynote talks at major international conferences. In 2007, he received the Award of the Chairman of the Czech Science Foundation for the Best Research Project and the Prize of the Academy of Sciences of the Czech Republic for the contribution to image fusion theory. In 2010, he received by the prestigious SCOPUS 1000 Award presented by Elsevier.

Janne Heikkilä (SM'11) received the Doctor of Science in Technology degree in information engineering from the University of Oulu, Oulu, Finland, in 1998. Currently, he is a Professor of information technology with the Department of Computer Science and Engineering, University of Oulu, and an Associate Leader of the Center for Machine Vision Research. He has served on committees of several international conferences and as a reviewer in many scientific journals. He is an Associate Editor of *IET Computer Vision*, a Governing Board Member of the International Association for Pattern Recognition. From 2006 to 2009, he was the President of the Pattern Recognition Society of Finland. His current research interests include computer vision, pattern recognition, digital image and video processing, and statistical signal processing. He has contributed to more than 130 peer reviewed international scientific articles.